Chen *et al. Nanoscale Research Letters* (2019) 14:73
https://doi.org/10.1186/s11671-019-2893-2

Nanoscale Research Letters

NANO IDEA Open Access

Controllable Optical Bistability and Four-Wave Mixing in a Photonic-Molecule Optomechanics

Hua-Jun Chen*, Hong-Wei Wu, Jian-Yong Yang, Xue-Chao Li, Ya-Juan Sun and Yuan Peng

Abstract

We theoretically investigate the nonlinear optical phenomena including optical bistability and four-wave mixing (FWM) process in a composite photonic-molecule cavity optomechanical system. The photonic-molecule cavity consisted of two whispering gallery mode (WGM) microcavities, where one WGM cavity is an optomechanical cavity with high-cavity dissipation κ and the other WGM cavity is an auxiliary ordinary optical cavity with high-quality factor (Q). Controlling the parameters of the system, such as the coupling strength J between the two cavities, the decay rate ratio δ of the two cavities, and the pump power P, the optical bistability can be controlled. Furthermore, the FWM process which presents the normal mode-splitting is also investigated in the FWM spectrum under different parameter regimes. Our study may provide a further insight of nonlinear phenomena in the composite photonic-molecule optomechanic systems.

Keywords: Photonic-molecule optomechanics, Optical bistability, Four-wave mixing

Background

Optomechanic systems (OMS) [1], consisting of optical cavities coupled to mechanical resonators and exploring radiation pressure-induced coherent photon-phonon interactions, have recently attracted much attention because they offer a platform to manipulate mechanical resonators and electromagnetic fields, and pave the way for potential applications of optomechanical devices, such as phonon laser [2, 3], sensing [4], phonon squeezing [5], the realization of squeezed light [6–8], ground-state cooling [9–11], and optomechanically induced transparency (OMIT) [12–15]-induced store light in solid-state devices [16, 17]. Although most attention has been paid to the single OMS, to realize compound OMS by integrating more optical or mechanical modes such as one mechanical mode coupled to two optical modes via radiation pressure [18, 19] and the phononic interaction between two mechanical resonators [20, 21] become a tendency for further investigating the OMS and their potential applications in quantum information processing. Based on the hybrid compound OMS, the transfer of a quantum state [22], OMIT-like phonon cooling [23], optomechanical dark mode [24], and phonon-mediated electromagnetically induced absorption [25] has been researched widely. In the numerous compound OMS, as a natural extension of the generic OMS, two directly coupled whispering gallery mode (WGM) microcavities termed photonic-molecule [26, 27] with optomechanical effect in one WGM microcavity have attracted much attention. There are two kinds of interplay in the compound photonic-molecule optomechanical system: the first one is the optomechanical interaction induced by the radiation pressure and the other one is cavity-cavity coupling via tunable photon tunneling. The two interactions together give rise to several interesting phenomena including phonon lasing [2, 3], chaos [28], ground-state cooling [23], and coherent control of light transmission [25, 29, 30].

On the other hand, OMS also provide a platform to investigate the nonlinear effect of light-matter interaction. Among all the nonlinear phenomena in OMS, optical bistability and four-wave mixing (FWM) are typical nonlinear optical phenomenon focusing on researchers' interest. In recent year, the bistable behavior of the mean intracavity photon number has been extensively studied

*Correspondence: chenphysics@126.com
School of Mechanics and Photoelectric Physics, Anhui University of Science and Technology, Huainan Anhui 232001, China

in various OMS, such as Bose-Einstein condensate cavity optomechanical system [31, 32], OMS with a quantum well [33], ultracold atoms [34, 35], and other hybrid OMS [36, 37]. In addition, FWM can be described as the cavity driven by a strong pump laser with frequency ω_p and a weak probe laser frequency ω_s, and then, two pump photons would mix with a probe photon via the mechanical mode to yield an idler photon at frequency $2\omega_p - \omega_s$ in OMS, and it is also investigated in previous works, such as the mode-splitting in strong coupling optomechanical system [38], coherent mechanical driving OMS [39, 40], and a two-mode cavity optomechanical system [41]. However, optical bistability and FWM have been seldom studied in composite photonic-molecule OMS, where the coupling strength represented by J of the two cavities play a key role affecting these nonlinear optical phenomena.

In the present work, we consider a composite photonic-molecule cavity optomechanical system, consisted of two WGM microcavities, where one WGM cavity is an optomechanical cavity with high-cavity dissipation κ, and the other WGM cavity is an auxiliary ordinary optical cavity with high-quality factor (Q) [42]. As Liu et al. [43] demonstrated, it remains difficult to achieve high Q factor and small mode volume (V) simultaneously for the same type of resonator. In the photonic-molecule optomechanics, by coupling the originally optomechanical cavity c with high-cavity dissipation κ (without high Q) to an auxiliary cavity mode a with high Q but large V, the requirement for high Q and small V for the same cavity can be removed. We introduce a ratio parameter $\delta = \kappa_c/\kappa_a$, where $\kappa_c = \omega_c/Q_c$ and $\kappa_a = \omega_a/Q_a$ are the decay rates of cavity modes c and a (ω_c and ω_a are the frequencies of cavity c and a) to investigate the nonlinear effect in the photonic-molecule optomechanics. Here, the optomechanical cavity c is driven by the pump laser while the auxiliary cavity a is driven by the probe laser. The cavity c is coupled to cavity a via evanescent field, and the coupling strength J between the two cavities can be controlled by varying the separation between the two WGM cavities [26]. We investigate the optical bistability and FWM based on the composite photonic-molecule OMS by varying the coupling strength J between the cavity resonators, and a tunable and controllable optical bistability and FWM can be achieved with manipulating the coupling strength J between the two cavities. Further, with adjusting the parameter δ and the pump power P, the FWM process can be controlled.

Model and Theory

The photonic-molecule optomechanics is shown in Fig. 1. The first cavity supports an optical mode c with the frequency ω_c driven by the pump laser with frequency ω_p and the amplitude $\varepsilon_p = \sqrt{P/\hbar\omega_p}$. The radiation pressure induces a mechanical mode b with the mechanical resonator frequency ω_m, and the single-photon optomechanical coupling rate is $g = g_0 x_0$ ($g_0 = \omega_c/R$ and R is the radius of cavity c), and the zero-point fluctuation of the

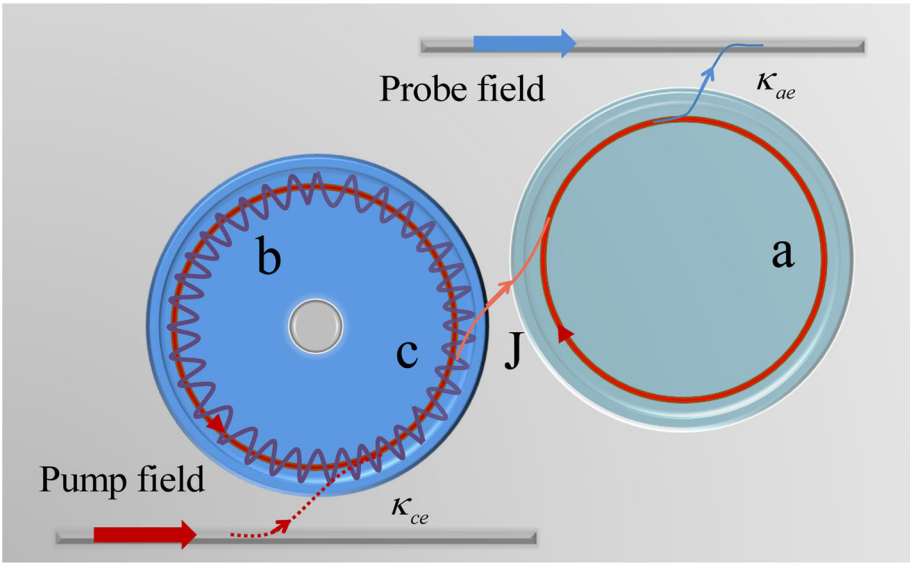

Fig. 1 Schematic diagram of the composite photonic-molecule cavity optomechanical system including two WGM cavities. The first WGM cavity with high-cavity dissipation κ is optomechanical cavity c driven by a pump laser, and radiation pressure force induces the mechanical mode b coupling to cavity c with coupling strength g. The second WGM cavity a is an auxiliary cavity driven by a probe laser with high-quality factor (Q). The optomechanical cavity c is coupled to cavity a via evanescent field, and we introduce a parameter J to describe the coupling strength of the two cavities, which can be controlled by varying the separation between them [26]

mechanical oscillator's position is $x_0 = \sqrt{\hbar/2M\omega_m}$ [13]. Then, the Hamiltonian of optomechanics c is [13]

$$H_c = \hbar\Delta_c c^\dagger c + \hbar\omega_m b^\dagger b - \hbar g a^\dagger a\left(b^\dagger + b\right) + i\hbar\sqrt{\kappa_{ce}}\varepsilon_p\left(c^\dagger - c\right), \tag{1}$$

where $\Delta_c = \omega_c - \omega_p$ is the detuning of the pump field and cavity c. c and $c^\dagger$ represent the bosonic annihilation and creation operators of the cavity mode c, and $b^\dagger(b)$ is the creation (annihilation) operator of mechanical mode. The auxiliary cavity only supports an optical mode a driven by the probe laser with frequency ω_s, and its amplitude ε_s is $\varepsilon_s = \sqrt{P_s/\hbar\omega_s}$. We introduce the annihilation and creation operators a and $a^\dagger$ to describe the cavity a, and its Hamiltonian is [13]

$$H_a = \hbar\Delta_a a^\dagger a + i\hbar\sqrt{\kappa_{ae}}\varepsilon_s\left(a^\dagger e^{-i\Omega t} - a e^{i\Omega t}\right) \tag{2}$$

where $\Delta_a = \omega_a - \omega_p$ is the detuning of the pump field and cavity a, and $\Omega = \omega_s - \omega_p$ is the pump-probe detuning. We use two tapered fibers to excite the cavity mode a and cavity mode c as the optical waveguide with the coupling rate κ_{ae} and κ_{ce}. The optomechanical cavity c couples to cavity a through an evanescent field, and the cavity-cavity coupling rate J can be efficiently tuned by changing the distance between them [26]. When the coupling strength J is weak in between the two cavities, then the energy from cavity c cannot transfer easily to cavity a. Conversely, if the coupling strength J increases with decreasing the distance between the two cavities, then the energy can easily flow from the two cavities. The linearly coupled interaction between the two cavities is described by [26] $\hbar J\left(a^\dagger c + a c^\dagger\right)$. Then, the total Hamiltonian in the rotating wave frame of pump frequency ω_c can be written [3, 13, 23]

$$\begin{aligned} H =& \hbar\Delta_a a^\dagger a + \hbar\Delta_c c^\dagger c + \hbar\omega_m b^\dagger b + \hbar J\left(a^\dagger c + a c^\dagger\right) - \hbar g a^\dagger a\left(b^\dagger + b\right) \\ &+ i\hbar\sqrt{\kappa_{ce}}\varepsilon_p\left(c^\dagger - c\right) + i\hbar\sqrt{\kappa_{ae}}\varepsilon_s\left(a^\dagger e^{-i\Omega t} - a e^{i\Omega t}\right). \end{aligned} \tag{3}$$

The decay rate of the two cavities mode $\kappa = \kappa_c = \kappa_a = \kappa_{ex} + \kappa_0$ with the intrinsic photon loss rate κ_0, and κ_{ex} describes the rate at which energy leaves the optical cavity into propagating fields [13]. Here, for simplicity, we only consider the condition of $\kappa_{ex} = \kappa_0 = \kappa_{ae} = \kappa_{ce}$, and we consider $\omega_c = \omega_a$.

We use the Heisenberg equation of motion $i\hbar\partial_t O = [O, H]$ $(O = a, c, X)$ and introduce corresponding damping and noise operators, and we obtain the quantum Langevin equations as follows [44]:

$$\partial_t a = -(i\Delta_a + \kappa_a)a - iJc + \sqrt{\kappa_{ae}}\varepsilon_s e^{-i\Omega t} + \sqrt{2\kappa_a}a_{\text{in}}, \tag{4}$$

$$\partial_t c = -(i\Delta_c + \kappa_c)c + igcX - iJa + \sqrt{\kappa_{ce}}\varepsilon_p + \sqrt{2\kappa_c}c_{\text{in}}, \tag{5}$$

$$\partial_t^2 X + \gamma_m\partial_t X + \omega_m^2 X = 2g\omega_m c^\dagger c + \xi, \tag{6}$$

where $X = b^\dagger + b$ is the position operator and γ_m is the decay rate of the resonator. a_{in} and c_{in} describing the Langevin noises follow the relations [45]

$$\left\langle a_{\text{in}}(t)a_{\text{in}}^\dagger\left(t'\right)\right\rangle = \left\langle c_{\text{in}}(t)c_{\text{in}}^\dagger\left(t'\right)\right\rangle = \delta\left(t - t'\right), \tag{7}$$

$$\langle a_{\text{in}}(t)\rangle = \langle c_{\text{in}}(t)\rangle = 0. \tag{8}$$

The resonator mode is influenced by stochastic force process with the following correlation function [46]

$$\left\langle \xi^\dagger(t)\xi\left(t'\right)\right\rangle = \frac{\gamma_m}{\omega_m}\int\frac{d\omega}{2\pi}\omega e^{-i\omega\left(t-t'\right)}\left[1 + \coth\left(\frac{\hbar\omega}{2\kappa_B T}\right)\right], \tag{9}$$

where k_B is Boltzmann constant and T indicates the reservoir temperature.

When the optomechanical cavity c is driven by a strong pump laser, the Heisenberg operator can be divided into two parts, i.e., steady-state mean value O_0, and small fluctuation δO with zero mean value $\langle\delta O\rangle = 0$. The steady-state values determine the intracavity photon numbers $\left(n_a = |a_s|^2 \text{ and } n_c = |c_s|^2\right)$ determined by

$$n_c = \frac{\kappa_{ce}\varepsilon_p^2\left(\Delta_a^2 + \kappa_a^2\right)}{\left(\Delta'^2 + \kappa_c^2\right)\left(\Delta_a^2 + \kappa_a^2\right) + 2J^2\left(\kappa_a\kappa_c - \Delta'\Delta_a\right) + J^4}, \tag{10}$$

$$n_a = \frac{\kappa_{ce}\varepsilon_p^2 J^2}{\left(\Delta'^2 + \kappa_c^2\right)\left(\Delta_a^2 + \kappa_a^2\right) + 2J^2\left(\kappa_a\kappa_c - \Delta'\Delta_a\right) + J^4}, \tag{11}$$

where $\Delta' = \Delta_c - 2g^2 n_c/\omega_m$. This form of coupled equations are characteristic of the optical bistability. In the following section, we will discuss the parameters such as the pump power P , the cavity-cavity coupling strength J, and the ratio parameter δ that affect the optical bistability. Keeping only the linear terms of the fluctuation operators and making the ansatz [47] $\langle\delta a\rangle = a_+ e^{-i\Omega t} + a_- e^{i\Omega t}$, $\langle\delta c\rangle = c_+ e^{-i\Omega t} + c_- e^{i\Omega t}$, $\langle\delta X\rangle = X_+ e^{-i\Omega t} + X_- e^{i\Omega t}$, we then obtain

$$a_- = \frac{\Lambda_1}{\Lambda_2 - \Lambda_3}, \tag{12}$$

where $\Lambda_1 = igc_s^2\eta^* J^2\varepsilon_s\sqrt{\kappa_{ae}}$, $\Lambda_2 = (i\Delta_{a2} + \kappa_a)(i\Delta_2 + \kappa_c)[(i\Delta_1 - \kappa_c)(i\Delta_{a1} - \kappa_a) - J^2]$, $\Lambda_3 = -g^2\eta^{*2}n_c^2(i\Delta_{a1} - \kappa_a)(i\Delta_{a2} + \kappa_a)$, $\Delta_{a1} = \Delta_a - \Omega$, $\Delta_{a2} = \Delta_a + \Omega$, $\Delta_1 = \Delta' - \Omega + g\eta n_c$, $\Delta_2 = \Delta' + \Omega + g\eta^* n_c$, and $\eta = 2g\omega_m/(\omega_m^2 - i\gamma_m\Omega - \Omega^2)$. Using the standard input-output relation [45]

$a_{\text{out}}(t) = a_{\text{in}}(t) - \sqrt{2\kappa_a}a(t)$, where $a_{\text{out}}(t)$ is the output field operator, and obtain the expectation value of the output fields:

$$\begin{aligned} a_{\text{out}}(t) &= (\varepsilon_p - \sqrt{\kappa_{ae}}a_s)e^{-i\omega_p t} + (\varepsilon_s - \sqrt{\kappa_{ae}}a_+)e^{-i(\delta+\omega_p)t} - \sqrt{\kappa_{ae}}a_- e^{-i(\delta-\omega_p)t} \\ &= (\varepsilon_p - \sqrt{\kappa_{ae}}a_s)e^{-i\omega_p t} + (\varepsilon_s - \sqrt{\kappa_{ae}}a_+)e^{-i\omega_s t} - \sqrt{\kappa_{ae}}a_- e^{-i(2\omega_p-\omega_s)t} \end{aligned} \tag{13}$$

where $a_{\text{out}}(t)$ is the output field operator. Equation (13) shows that the output field consists of three terms. The first term corresponds to the output field at driving field with amplitude ε_p and frequency ω_p. The second term corresponds to the probe field with frequency ω_s related to the anti-Stokes field resulting in OMIT, which has been investigated in various optomechanical systems [12–15, 48]. The last one corresponds to the output field with frequency $2\,\omega_p - \omega_s$ related to the stoke field displaying the FWM. In the FWM process, the two photons of the driving field interact with a single photon of the probe field each with frequencies ω_p and ω_s born a new photon of frequency $2\,\omega_p - \omega_s$. The FWM intensity in terms of the probe field can be defined as [49]

$$\text{FWM} = \left|\frac{\sqrt{\kappa_{ae}}a_-}{\varepsilon_s}\right|^2, \tag{14}$$

which is determined by the optomechanical coupling strength g, the pump power P, the cavity-cavity coupling strength J, and the decay rate ratio δ of the two cavities.

Numerical Results and Discussions

In this section, we first investigate the bistable behavior of the steady-state photon number n_c and n_a of the two cavities according to Eqs. (10) and (11). Because it is too cumbersome to give the analytical expression of the bistability condition, here we will present the numerical results. We choose the parameters similar to those in Ref. [13, 26] : the parameters of cavity c as [13]: $g_0 = 12$ GHz/nm, $\gamma_m = 41$ kHz, $\omega_m = 51.8$ MHz, $\kappa_c = 5$ MHz, $m = 20$ ng, $\lambda = 750$ nm, and $Q = 1500$, and the order of magnitude of the pump power is milliwatt (1 mW$= 10^{-3}$ W). For cavity a, we consider $\omega_a = \omega_c$ and $\kappa_c = \kappa_a$. The coupling strength J between the two cavity modes plays a key role and can affect the bistable behavior and FWM. It has been reported experimentally that the coupling strength J depends on the distance between cavity c and cavity a [26] (also the coupling strength decreases exponentially with increasing the distance of the two cavities). Here, we expect the coupling strength $J \sim \sqrt{\kappa_c\kappa_a}$.

Equations (10) and (11) giving the intracavity photon numbers of optomechanical cavity c and ordinary cavity a are coupled cubic equations, which exhibit bistable behavior. We first consider the condition of $J = 0$, i.e., only a single optomechanical cavity c, and Fig. 2a plots the mean intracavity photon number n_c of optomechanical cavity c as a function of the cavity-pump detuning $\Delta_c = \omega_c - \omega_p$ with three pump powers. When the pump

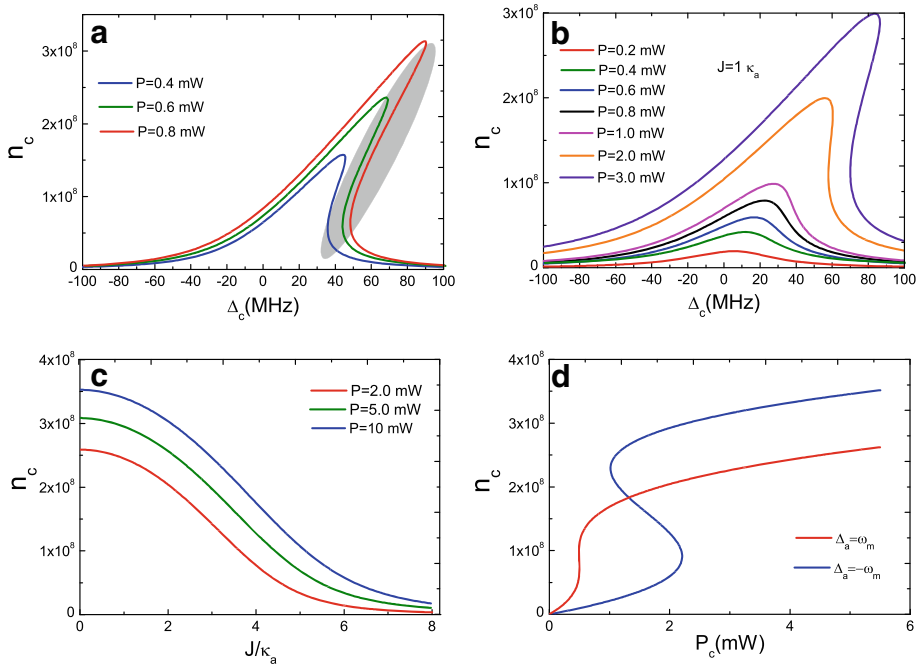

Fig. 2 a Mean intracavity photon number of optomechanical cavity c as a function of the cavity-pump detuning Δ_c with three pump powers at $J = 0$. **b** Mean intracavity photon number of optomechanical cavity c as a function of the cavity-pump detuning Δ_c with several different pump powers under $J = 1.0\,\kappa_a$. **c** Mean intracavity photon number n_c of optomechanical cavity c as a function of J with three pump powers. **d** Mean intracavity photon number n_c as a function of P for $\Delta_c = \Delta_a = \omega_m$

power is less than $P = 0.4$ mW (such as $P = 0.1$ mW), the curve is nearly Lorentzian. With increasing the power P to a critical value, the optomechanical cavity c exhibits bistable behavior, as shown in the curves for $P = 0.4$ mW to $P = 0.8$ mW, where the initially Lorentzian resonance curve becomes asymmetric. The mean intracavity photon number n_c has three real roots (Eq. (10)), and the largest and smallest roots are stable, and the middle one is unstable, which is represented in an oval in Fig. 2a. However, when we consider the optical cavity a, i.e., $J \neq 0$ such as $J = 1.0\ \kappa_a$, the bistable behavior is broken in some ways as shown in Fig. 2b. That is because when optomechanical cavity c coupled to optical cavity a, parts of intracavity photon number n_c of optomechanical cavity c will coupled into optical cavity a, and therefore, intracavity photon number n_c will decrease and then result in a destroyed bistable behavior. Figure 2c shows the mean intracavity photon number n_c of optomechanical cavity c as a function of the cavity-cavity coupling strength J with three pump powers. Obviously, the mean intracavity photon number n_c depends on the pump power P, and the intracavity photon number n_c is always decreasing with the increasing coupling strength J because parts of photon number are coupled into optical cavity a. Further, larger cavity-pump detuning is beneficial to observe the optical bistable behavior with increasing pump power P. Figure 2d plots the mean intracavity photon number n_c versus the pump power P with cavity a at red sidebands ($\Delta_a = \omega_m$) and blue sidebands ($\Delta_a = -\omega_m$), respectively, and the bistability presents the hysteresis loop behavior [50]. However, our results are different from the previous work of two-mode optomechanical system without considering the cavity-cavity coupling J. Therefore, the coupling strength J plays an important role in the bistability.

We further investigate bistable behavior of optical cavity a with Eq. (11). Figure 3a gives the intracavity photon number n_a of ordinary cavity a as a function of the cavity-pump detuning $\Delta_a = \omega_a - \omega_p$ with pump powers $P = 0.1$ mW, $P = 1.0$ mW, and $P = 10$ mW at $J = 1.0\,\kappa_a$. It is obvious that optical cavity a cannot behave as bistable behavior due to intracavity photon number n_a of cavity a from cavity c cannot maintain bistability in low-pump power. Actually, only high-pump power P can cavity a present bistable behavior, because only high-pump power driven optomechanical cavity c, much more photon number can couple into optical cavity a. We also plot the mean intracavity photon number n_a of optical cavity a as a function of the coupling strength J under three pump powers as shown in Fig. 3b. It is clear that when $J = 0$, $n_a = 0$, because there is no coupling between the two cavities at $J = 0$, and at this condition, no photon couples into optical cavity a. With increasing the coupling strength J (decreasing the distance of the

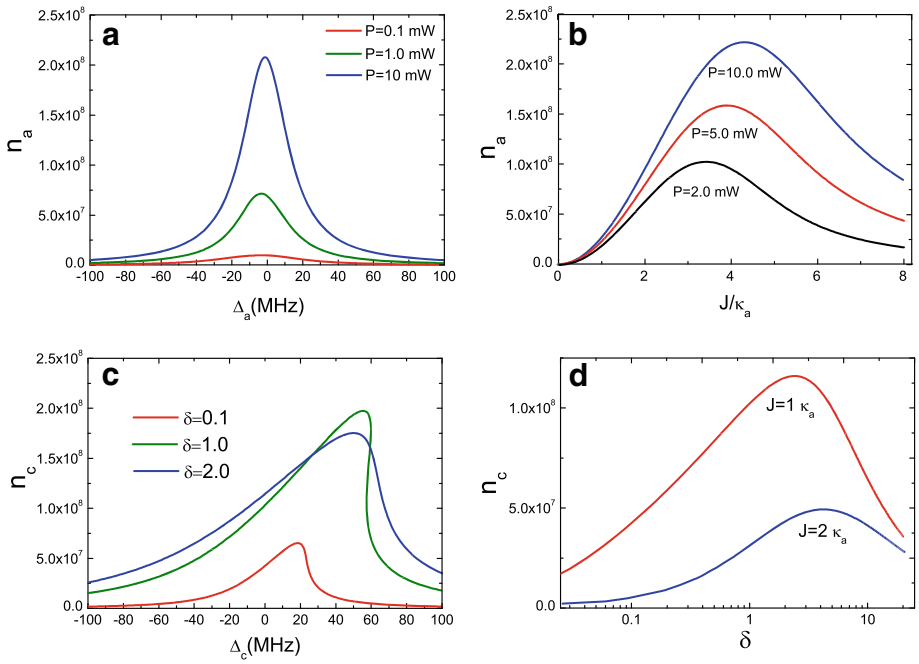

Fig. 3 a Mean intracavity photon number of ordinary cavity a as a function of the cavity-pump detuning Δ_a with three pump powers at $J = 1.0\,\kappa_a$. **b** Mean intracavity photon number n_a as a function of J with three pump powers. **c** Mean intracavity photon number n_c as a function of Δ_c with three ratio parameters δ. **d** Mean intracavity photon number n_c as a function of δ for two J

two cavities [26]), the intracavity photon numbers n_a of ordinary optical cavity a increase but not always. There is an optimum coupling strength J for the maximum value of n_a under different pump power, and then, n_a will decrease with the increasing J . It is a remarkable fact that the coupling strength J between the two cavities can be adjusted [26].

In addition, we consider a ratio parameter $\delta = \kappa_c/\kappa_a$ ($\kappa_c = \omega_c/Q_c$ and $\kappa_a = \omega_a/Q_a$) to investigate the parameters of the two cavities that influence bistable behavior. κ is the decay rate of the cavity mode, which is related to the frequency and quality factor of the cavity. As we know, it is difficult to achieve high Q and small V simultaneously for a cavity mode due to the diffraction limit. For an optical cavity, a smaller V corresponding to a larger radiative decay rate results in a lower Q. Although different types of cavities possess their own unique properties, the weigh between high Q and small V still exists. However, when by coupling the originally OMS c with high-cavity dissipation to an auxiliary cavity mode a with high Q but large V, the bistable behavior will change significantly. Figure 3c shows the mean intracavity photon number n_c of optomechanical cavity c as a function of Δ_a under several different $\delta = \kappa_c/\kappa_a$ with an unchanged coupling strength $J = 1.0\ \kappa_a$. We can find that the bistable behavior can appear, but the intracavity photon number n_c is small at $\delta = 0.1$ with $J = 2\ \kappa_a$, i.e., $\kappa_c = 0.1\ \kappa_a$ which means $Q_c > Q_a$. When increasing the ratio δ from $\delta = 1.0$ to $\delta = 2.0$, the intracavity photon number n_c experiences the change from bistable behavior to nearly Lorentzian line profile. That is to say when $Q_c < Q_a$, the bistable behavior will be broken, but there is an optimal condition, i.e., $Q_c = Q_a$. In Fig. 3d, we give the intracavity photon number n_c as a function of δ with two different J, and obviously, in increasing the ratio parameter δ, the intracavity photon numbers n_c increase. When it reaches an optimum value for a given J, then n_c decrease. Therefore, controlling the cavity parameters, like the decay rate κ or the quality factor of the cavities, the bistable behavior can be controlled.

On the other hand, as a typical nonlinear optical phenomenon, we also investigate the FWM process with Eq. (14) in the photonic-molecule optomechanical system. Figure 4 plots the FWM spectrum as a function of the probe-cavity a detuning $\Delta_s = \omega_s - \omega_a$ at $\Delta_a = \Delta_c = 0$ under different parameter regimes. Figure 4a–d displays the FWM spectra evolution under different pump power P at $J = 1.0\ \kappa_a$. It is clear that the FWM spectra present three peaks, where a Lorentzian peak near $\Delta_s = 0$ and two mode-splitting peaks locate at $\pm\omega_m$, and

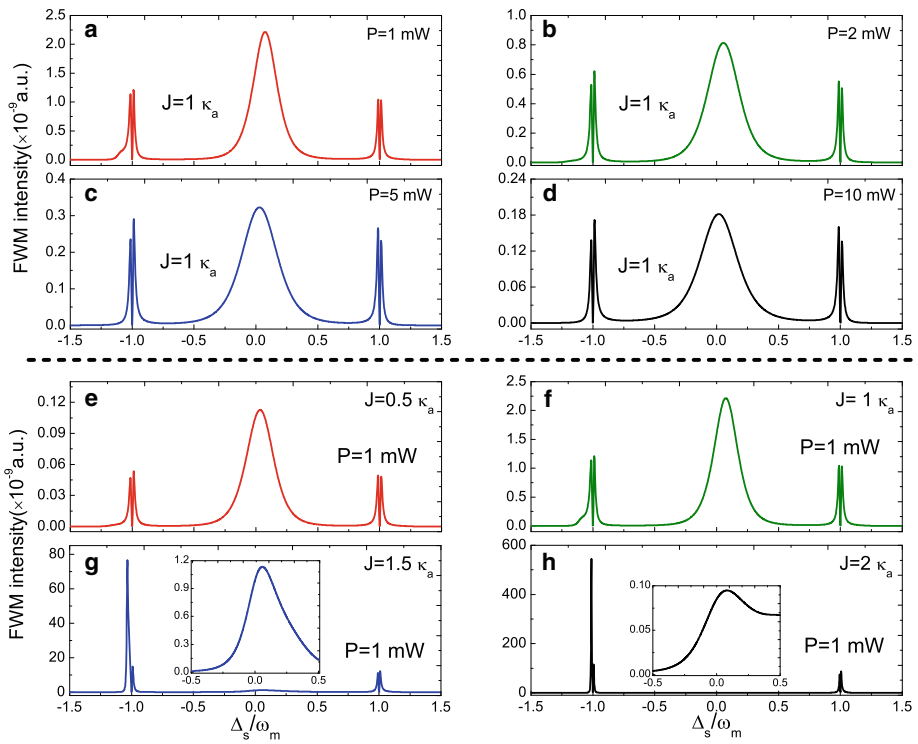

Fig. 4 a–d FWM intensity as a function of the normalized probe-pump detuning Δ_s for different pump power at $J = 1.0\ \kappa_a$. **e–h** FWM intensity as a function of Δ_s for different J at pump power $P = 1.0$ mW

the FWM intensity decreases with increasing the pump power. Figure 4e–h shows the change of FWM spectra from $J = 0.5\ \kappa_a$ to $J = 2.0\ \kappa_a$ at pump power $P = 1.0$ mW. With increasing the coupling strength J from $J = 0.5\ \kappa_a$ to $J = 2.0\ \kappa_a$, the FWM spectra change significantly. The phenomena can be explained with a dressed-state picture which has demonstrated in single cavity optomechanical system [51].

We then investigate the FWM spectra at $\Delta_a = \Delta_c \neq 0$. Figure 5a–d gives the FWM spectra at the red sideband, i.e., $\Delta_a = \Delta_c = \omega_m$ under an unchanged $J = 1.0\ \kappa_a$ with increasing the pump power from $P = 1.0$ to $P = 10$ mW. Two normal mode-splitting peaks appear in the FWM spectra locating at $\pm\omega_m$ respectively, and the FWM intensity decreases with increasing the pump power. Figure 5e–h shows the FWM spectra at the red sideband, i.e., $\Delta_a = \Delta_c = \omega_m$ under a fixed pump power $P = 2.0$ mW with increasing the coupling strength J from $J = 0.5\ \kappa_a$ to $J = 2.0\ \kappa_a$. Obviously, the FWM intensity increases with increasing the coupling strength J, and the bigger J means more photon numbers coupled into optical cavity a. When changing the detuning Δ_a and Δ_c from the red sideband to the blue sideband, i.e., $\Delta_a = \Delta_c = -\omega_m$, the evolution of the FWM spectra change prominently. Figure 5i–l displays the FWM spectra at blue sideband under four different pump powers, and the FWM intensity decreases with increasing the pump power even at the blue sideband. Except two normal mode-splitting peaks locating at $\pm\omega_m$, there are also two sharp sideband peaks appear in the FWM spectra and their location are related to the pump power. In Fig. 5m–p, we also discuss the coupling strength J that affect the FWM spectra under the blue sideband. Whether other sharp sideband peaks appear in the FWM spectra depend on the the coupling strength J.

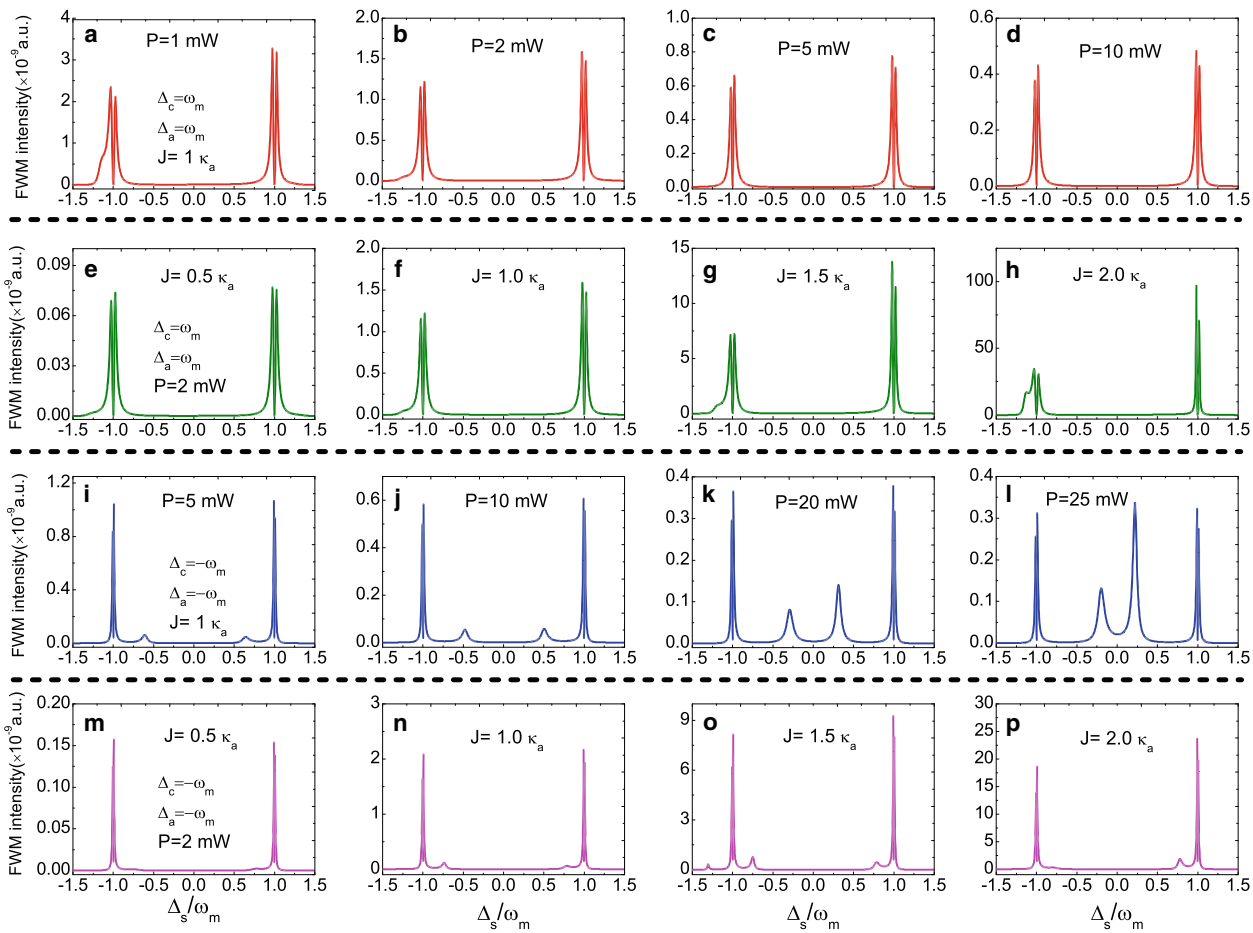

Fig. 5 a–d FWM intensity as a function of Δ_s for different pump power P at the red sideband ($\Delta_c = \Delta_a = \omega_m$) and $J = 1.0\ \kappa_a$. **e–h** FWM intensity as a function of Δ_s for different J under the red sideband and the pump power $P = 2.0$ mW. **i–l** FWM intensity as a function of Δ_s for different pump power P at the blue sideband ($\Delta_c = \Delta_a = -\omega_m$) and $J = 1.0\ \kappa_a$. **m–p** FWM intensity as a function of Δ_s for different J under the blue sideband and the pump power $P = 2.0$ mW

Further, since the ratio parameter $\delta = \kappa_c/\kappa_a$ can influence the intracavity photon number in the composite photonic-molecule OMS, the FWM spectra can be manipulated with controlling the parameter δ. Figure 6a–h presents the FWM spectra at unchanged parameters $J = 2.0\ \kappa_a$ and $P = 10$ mW under the red sideband with increasing the ratio δ from $\delta = 0.05$ to $\delta = 3.0$, and the FWM intensity decreases with increasing the ratio δ. While in the blue sideband, other sharp sideband peaks will appear in the FWM spectra as shown in Fig. 6i–p, and the FWM intensity also decreases with increasing the ratio δ. Therefore, with controlling the cavity parameters, like the decay rate κ or the Q of the cavities, the FWM can achieve straightforward in the composite photonic-molecule OMS.

Conclusion

We have investigated the optical bistability and four-wave mixing in a composite WGM cavity photonic-molecule optomechanical system, which includes an optomechanical cavity with high-cavity dissipation coupled to an auxiliary cavity with high-quality factor. We investigate the optical bistability under different parameter regimes such as the coupling strength J between the two cavities and the decay rate ratio δ of the two cavities in the system. The optical bistability can be adjusted by the pump field driving the optomechanical cavity, and the intracavity photon number in the two cavities is determined by the coupling strength J. Further, we have also demonstrated how to control the FWM process in the photonic-molecule optomechanical system under different driving conditions (the red sideband and the blue sideband) and different parameter conditions (the coupling strength J and the ratio δ). Numerical results show that the FWM process can be controlled with such parameters. These results are beneficial for better understanding the nonlinear phenomena in the composite photonic-molecule optomechanical system.

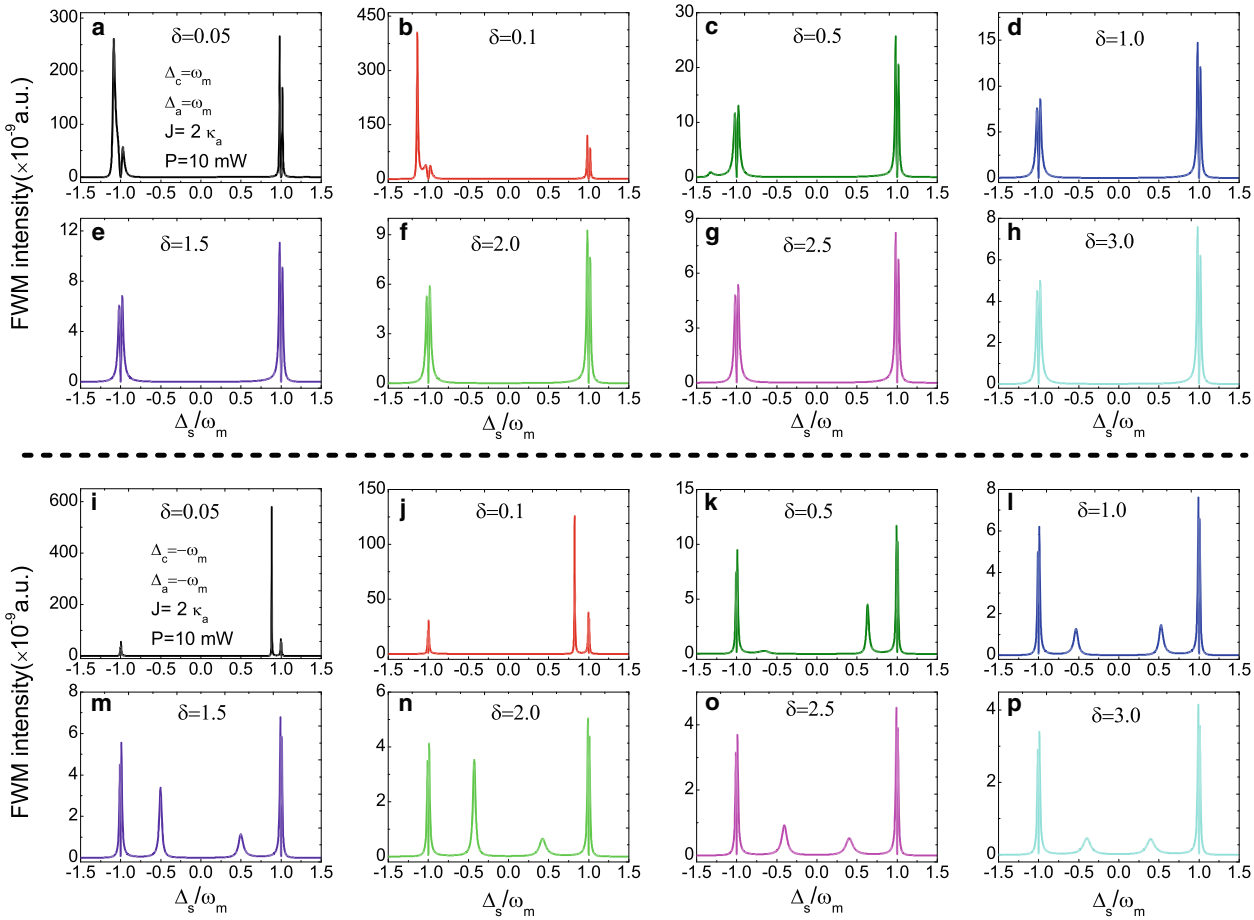

Fig. 6 a–h FWM intensity as a function of Δ_s for several different ratio parameters δ at the red sideband ($\Delta_c = \Delta_a = \omega_m$) and $J = 2.0\ \kappa_a$, $P = 10$ mW. **i–p** FWM intensity as a function of Δ_s for several different ratio parameters δ at the blue sideband ($\Delta_c = \Delta_a = -\omega_m$) and $J = 2.0\ \kappa_a$, $P = 10$ mW

Abbreviations
C-OMS: Cavity optomechanics systems; FWM: Four-wave mixing; OMS: Optomechanics systems; OMIT: Optomechanically induced transparency; Q: Quality; V: Volume; WGM: Whispering gallery mode

Acknowledgements
The authors gratefully acknowledge support from the National Natural Science Foundation of China (Nos:11647001 and 11804004) and Anhui Provincial Natural Science Foundation (No:1708085QA11). We acknowledge Lan Yang at Washington University for helpful suggestion in a meeting of "Microcavity Photonics".

Funding
Hua-Jun Chen is supported by the National Natural Science Foundation of China (Nos:11647001 and 11804004) and Anhui Provincial Natural Science Foundation (No:1708085QA11).

Availability of data and materials
The photonic-molecule optomechanical cavity system is demonstrated by Yang in Ref. [26], and the optomechanical model and parameters are investigated by Weis in Ref. [13].

Authors' contributions
HJC finished the main work of this paper, including conceiving of the idea, deducing the formulas, plotting the figures, and drafting the manuscript. HWW, XCL, JYY, YJS, and YP participated in the discussion and provided some useful suggestion. All authors are involved in revising the manuscript. All authors read and approved the final manuscript.

Competing interests
The authors declare that they have no competing interests.

Publisher's Note

Received: 22 November 2018 Accepted: 5 February 2019
Published online: 01 March 2019

References
1. Aspelmeyer M, Kippenberg TJ, Marquardt F (2014) Cavity optomechanics. Rev Mod Phys 86(4):1391
2. Grudinin IS, Lee H, Painter O, et al. (2010) Phonon laser action in a tunable two-level system. Phys Rev Lett 104(8):083901
3. Jing H, Özdemir SK, Lü XY, et al. (2014) PT-symmetric phonon laser. Phys Rev Lett 113(5):053604
4. Li JJ, Zhu KD (2013) All-optical mass sensing with coupled mechanical resonator systems. Phys Rep 525(3):223–254
5. Wollman EE, Lei CU, Weinstein AJ, et al. (2015) Quantum squeezing of motion in a mechanical resonator. Science 349(6251):952–955
6. Brooks DWC, Botter T, Schreppler S, et al. (2012) Non-classical light generated by quantum-noise-driven cavity optomechanics. Nature 488(7412):476
7. Safavi-Naeini AH, Grölacher S, Hill JT, et al. (2013) Squeezed light from a silicon micromechanical resonator. Nature 500(7461):185
8. Purdy TP, Yu PL, Peterson RW, et al. (2013) Strong optomechanical squeezing of light. Phys Rev X 3(3):031012
9. O'Connell AD, Hofheinz M, Ansmann M, et al. (2010) Quantum ground state and single-phonon control of a mechanical resonator. Nature 464(7289):697
10. Chan J, Alegre TPM, Safavi-Naeini AH, et al. (2011) Laser cooling of a nanomechanical oscillator into its quantum ground state. Nature 478(7367):89
11. Teufel JD, Donner T, Li D, et al. (2011) Sideband cooling of micromechanical motion to the quantum ground state. Nature 475(7356):359
12. Agarwal GS, Huang S (2010) Electromagnetically induced transparency in mechanical effects of light. Phys Rev A 81(4):041803
13. Weis S, Rivière R, Deléglise S, et al. (2010) Optomechanically induced transparency. Science 330(6010):1520–1523
14. Teufel JD, Donner T, Li D, et al. (2011) Sideband cooling of micromechanical motion to the quantum ground state. Nature 475(7356):359
15. Safavi-Naeini AH, Alegre TPM, Chan J, et al. (2011) Electromagnetically induced transparency and slow light with optomechanics. Nature 472(7341):69
16. Zhou X, Hocke F, Schliesser A, et al. (2013) Slowing, advancing and switching of microwave signals using circuit nanoelectromechanics. Nat Phys 9(3):179
17. Fan L, Fong KY, Poot M, et al. (2015) Cascaded optical transparency in multimode-cavity optomechanical systems. Nat Commun 6:5850
18. Hill JT, Safavi-Naeini AH, Chan J, et al. (2012) Coherent optical wavelength conversion via cavity optomechanics. Nat Commun 3:1196
19. Bai C, Hou BP, Lai DG, et al. (2016) Tunable optomechanically induced transparency in double quadratically coupled optomechanical cavities within a common reservoir. Phys Rev A 93(4):043804
20. Massel F, Cho SU, Pirkkalainen JM, et al. (2012) Multimode circuit optomechanics near the quantum limit. Nat Commun 3:987
21. Ma PC, Zhang JQ, Xiao Y, et al. (2014) Tunable double optomechanically induced transparency in an optomechanical system. Phys Rev A 90(4):043825
22. Wang YD, Clerk AA (2012) Using interference for high fidelity quantum state transfer in optomechanics. Phys Rev Lett 108(15):153603
23. Guo Y, Li K, Nie W, et al. (2014) Electromagnetically-induced-transparency-like ground-state cooling in a double-cavity optomechanical system. Phys Rev A 90(5):053841
24. Dong C, Fiore V, Kuzyk MC, et al. (2012) Optomechanical dark mode. Science 338(6114):1609–1613
25. Qu K, Agarwal GS (2013) Phonon-mediated electromagnetically induced absorption in hybrid opto-electromechanical systems. Phys Rev A 87(3):031802
26. Peng B, Özdemir ŞK, Lei F, et al. (2014) Parity–time-symmetric whispering-gallery microcavities. Nat Phys 10(5):394
27. Chang L, Jiang X, Hua S, et al. (2014) Parity–time symmetry and variable optical isolation in active–passive-coupled microresonators. Nat Photonics 8(7):524
28. Lü XY, Jing H, Ma JY, et al. (2015) P-T-symmetry-breaking chaos in optomechanics. Phys Rev Lett 114(25):253601
29. Jiang C, Liu H, Cui Y, et al. (2013) Electromagnetically induced transparency and slow light in two-mode optomechanics. Opt Express 21(10):12165–12173
30. Jing H, Özdemir ŞK, Geng Z, et al. (2015) Optomechanically-induced transparency in parity-time-symmetric microresonators. Sci Rep 5:9663
31. Brennecke F, Ritter S, Donner T, et al. (2008) Cavity optomechanics with a Bose-Einstein condensate. Science 322(5899):235–238
32. Yang S, Al-Amri M, Zubairy MS (2013) Anomalous switching of optical bistability in a Bose-Einstein condensate. Phys Rev A 87(3):033836
33. Sete EA, Eleuch H (2012) Controllable nonlinear effects in an optomechanical resonator containing a quantum well. Phys Rev A 85(4):043824
34. Kanamoto R, Meystre P (2010) Optomechanics of a quantum-degenerate Fermi gas. Phys Rev Lett 104(6):063601
35. Purdy TP, Brooks DWC, Botter T, et al. (2010) Tunable cavity optomechanics with ultracold atoms[J]. Phys Rev Lett 105(13):133602
36. Yan D, Wang ZH, Ren CN, et al. (2015) Duality and bistability in an optomechanical cavity coupled to a Rydberg superatom. Phys Rev A 91(2):023813
37. Xiong W, Jin DY, Qiu Y, et al. (2016) Cross-Kerr effect on an optomechanical system. Phys Rev A 93(2):023844
38. Huang S, Agarwal GS (2010) Normal-mode splitting and antibunching in Stokes and anti-Stokes processes in cavity optomechanics: radiation-pressure-induced four-wave-mixing cavity optomechanics. Phys Rev A 81(3):033830
39. Jia WZ, Wei LF, Li Y, et al. (2015) Phase-dependent optical response properties in an optomechanical system by coherently driving the mechanical resonator. Phys Rev A 91(4):043843
40. Xu XW, Li Y (2015) Controllable optical output fields from an optomechanical system with mechanical driving. Phys Rev A 92(2):023855
41. Jiang C, Cui Y, Liu H (2013) Controllable four-wave mixing based on mechanical vibration in two-mode optomechanical systems. Europhys Lett 104(3):34004

42. Chen HJ (2018) Manipulation of fast and slow light propagation by photonic-molecule optomechanics. J App Phys 124(15):153102
43. Liu YC, Luan X, Li HK, et al. (2014) Coherent polariton dynamics in coupled highly dissipative cavities. Phys Rev Lett 112(21):213602
44. Walls DF, Milburn GJ (1994) Quantum optics. Springer, Berlin
45. Gardiner CW, Zoller P (2000) Quantum noise. Springer, Berlin
46. Genes C, Vitali D, Tombesi P (2008) Emergence of atom-light-mirror entanglement inside an optical cavity. Phys Rev A 77(5):050307
47. Boyd RW (1992) Nonlinear optics. Academic, San Diego
48. Chen HJ (2018) Manipulation of fast and slow light propagation by photonic-molecule optomechanics. J Appl Phys 124(15):153102
49. Jiang C, Cui Y, Liu H (2013) Controllable four-wave mixing based on mechanical vibration in two-mode optomechanical systems. EPL (Europhys Lett) 104(3):34004
50. Jiang C, Liu H, Cui Y, et al. (2013) Controllable optical bistability based on photons and phonons in a two-mode optomechanical system. Phys Rev A 88(5):055801
51. Jiang C, Chen B, Li JJ, et al. (2011) Mass sensing based on a circuit cavity electromechanical system. J Appl Phys 110(8):083107